공학석사학위논문

하이브리드 차량의 주행 정보 기반 에너지 관리 전략에 대한 연구

A Study on Energy Management Strategy for Hybrid Electric Vehicles based on Driving Information

2019 년 8 월

서울대학교 대학원

기계항공공학부

심 재 욱

하이브리드 차량의 주행 정보 기반 에너지 관리 전략에 대한 연구

A Study on Energy Management Strategy for Hybrid Electric Vehicles based on Driving Information

지도교수 차 석 원

이 논문을 공학석사 학위논문으로 제출함

2019 년 4 월

서울대학교 대학원
기계항공공학부
심 재 욱

심재욱의 공학석사 학위논문을 인준함

2019 년 6 월

위 원 장 _____ 이 건 우

부위원장 _____ 차 석 원

위 원 _____ 안 성 훈

Abstract

A Study on Energy Management Strategy for Hybrid Electric Vehicles based on Driving Information

Jaeuk Sim
Department of Mechanical and Aerospace Engineering
Seoul National University

In this thesis, an energy management strategy (EMS) using prediction model based on driving information is proposed to improve the fuel efficiency of hybrid electric vehicle (HEV).

HEV uses both an engine and a motor, and is a representative eco-friendly vehicle with high fuel efficiency. To improve the efficiency of a HEV, the EMS of the supervisory controller that controls various powertrain components is very important. An equivalent consumption minimization strategy (ECMS) used in this study is a real-time optimization-based strategy that considers equivalent energy consumption of fuel and battery. A ECMS is easy to develop and have good real-time applicability, but a performance is largely dependent on the equivalent factor that equalize between the two energies. As with most optimization-based control strategies, the optimal equivalent factor can be obtained only when the entire future driving profile is known.

In this thesis, a method of changing the equivalent factor at every specific time period is used, and a prediction model that predicts the factor of the next time window through the current driving information is

proposed. The prediction model receives the time series data of the current time window driving information and several feature values extracted from it, and predicts an optimized equivalent factor for the next time window. The model was developed based on recurrent neural network (RNN) using long short-term memory (LSTM) and multi-layer perceptron (MLP). In order to prepare the data for the training of the prediction model, the cumulative driving information is divided into specific time windows, and the optimal equivalent factors for each time window are obtained based on the simulation. After training the prediction model using the collected data and testing it on separate data, it is confirmed that there is a high correlation between the predicted factor and the optimal factor. For the verification of vehicle simulation, the prediction model is combined with the EMS model using the ECMS to construct predictive-ECMS, and the forward simulation is performed using the vehicle and the driver model. Simulation results for test cycle showed less energy use compared to existing rule-based strategy and were more similar to the global optimized factor case.

The control strategy proposed in this thesis is an optimization-based control strategy that can improve the energy efficiency by using prediction model based on driving information. It is expected that the optimization -based control strategy will be realized through continuous research.

Keyword: Hybrid Electric Vehicle, Energy Management Strategy,
Equivalent Consumption Minimization Strategy,
Equivalent Factor Prediction, Driving Information

Student Number: 2017-28777

Contents

List of Figures

Chapter 1

Chapter 2

Chapter 3

Chapter 4

List of Tables

Chapter 2

Chapter 3

Chapter 4

Chapter 1. Introduction

1.1 Motivation

Over the past 100 years, the automobile industry has grown on the basis of fossil fuels, and most of the cars currently on the market are fueled by gasoline and diesel. However, the automotive industry has recently undergone a major change due to atmospheric environment issue. The number of vehicles in the world has greatly increased, and the environmental pollution problem caused by automobile exhaust gas is emerging. Major countries are actively pursuing efforts to curb emissions of pollutants in response to these atmospheric environmental problems. Figure 1.1 shows the regulation of carbon dioxide emissions in major countries [1]. In most countries, the regulation of carbon dioxide emissions after 2020 is expected to reach half of the early 2000s.

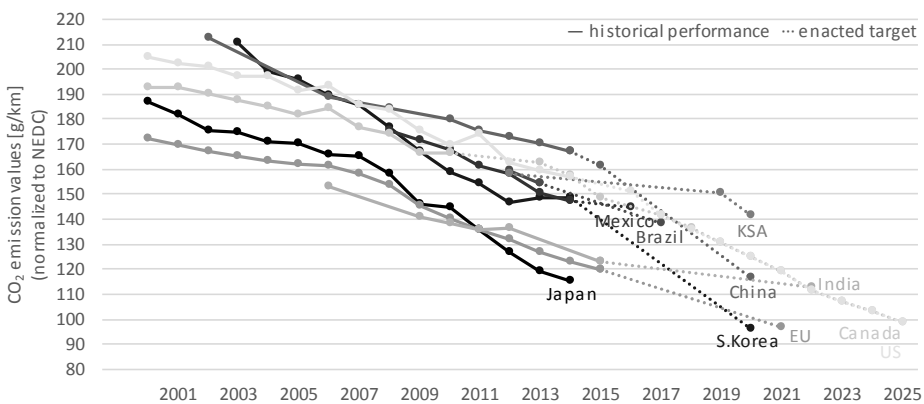

Figure 1.1 Historical fleet CO2 emissions performance and current standards for passenger cars [1]

In the automobile industry, which is highly dependent on fossil fuels, it is necessary to develop eco-friendly vehicles that can reduce the consumption of fossil fuels beyond the existing emission reduction technologies in order to cope with such environmental problems. Hybrid electric vehicle (HEV) or plug-in hybrid electric vehicle (PHEV) is becoming more popular as representative eco-friendly vehicle. Figure 1.2 shows the sales forecast of light duty vehicle according to BLUE Map scenario of international energy agency (IEA) [2]. According to the scenario, sales of HEVs and PHEVs will continue to increase from 2020 to 2040.

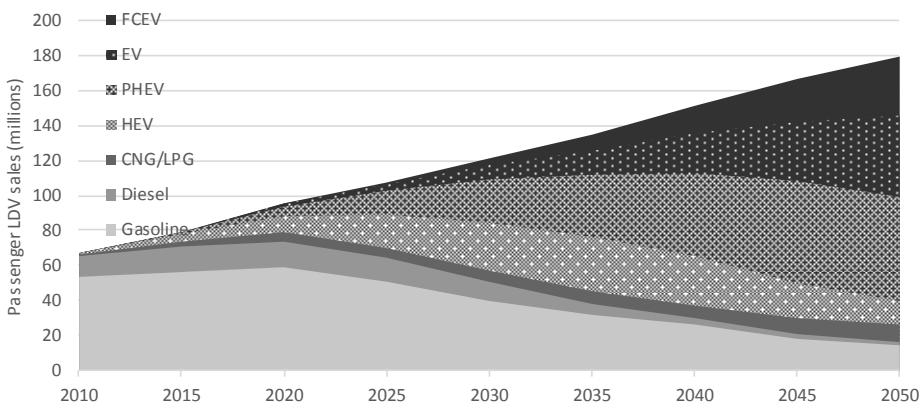

Figure 1.2 Annual light duty vehicle sales by technology type, International Energy Agency (IEA) BLUE Map scenario [2]

A hybrid vehicle is a vehicle that has two or more power sources for its operation. In general, a HEV is a vehicle equipped with an engine and a motor [3]. The HEV is more expensive than conventional vehicle due to various and complex powertrain components. The 48V mild hybrid powertrain is a good solution to this problem. HEVs are divided into mild hybrid, full hybrid and plug-in hybrid depending on the capacity of the battery and motor. The mild hybrid refers to a powertrain using a relatively

small battery and motor capacity. Especially, the mild hybrid powertrain using 48V component is a good system that can utilize the powertrain and chassis design of existing conventional vehicle as well as maximize the efficiency while reducing the increase of manufacturing cost.

The fuel economy of a HEV depends heavily on the supervisory energy management strategy (EMS), which controls the powertrain components such as the engine, transmission, motor, and battery. Therefore, researches for developing efficient EMS by applying various methods have been continuously carried out. Especially, in the case of mild HEV, it is essential to develop EMS that maximizes the hybridization effect compared to the conventional vehicle.

1.2 Background Studies

The EMS of the HEV is divided into a rule-based strategy and an optimization based strategy [4]-[5]. The rule-based strategy refers to all strategies that control the vehicle based on pre-defined control rules. It is applied to all HEVs currently on sale because it is the simplest and easiest to implement in real-time. Typically, there are deterministic rule-based methods [6]-[8] and fuzzy rule-based methods [9]-[11]. However, using a rule-based strategy does not provide optimal fuel economy and requires expert parameter tuning to improve fuel economy.

A typical optimization based strategy is dynamic programming (DP) [12]-[14]. DP is effective only when the entire driving velocity profile of the vehicle is known in advance, and real-time application is relatively difficult. Therefore, the DP is used for research purposes such as estimating the global optimal performance of the HEV for a specific driving profile, or for parameter tuning of a rule-based strategy [15]-[17].

Pontryagin's minimum principle (PMP) is also one of the optimization based control strategies [18]-[21]. In the case of PMP, real-time implementation is possible, but as in the case of DP, this global optimal control can be realized only when the overall driving velocity profile of the vehicle is known in advance.

As discussed above, various EMSs have been studied to improve the fuel efficiency of HEVs. However, all of these EMSs have tradeoffs between optimality and implementability, and all currently sold vehicles are using rule-based EMS that takes into account only implementability. Therefore, in this study, we try to develop EMS that can achieve high enough optimality while ensuring implementability.

The control strategy used in this study is based on an equivalent

consumption minimization strategy (ECMS) that belongs to an optimization based control strategy. A ECMS is an EMS using the relationship between fuel consumption and electric power consumption and was first introduced by G. Paganelli [22]-[23]. The underlying concept of ECMS is proved by PMP, and the theoretical background of ECMS is redefined in various studies [24]-[27]. As with the PMP, ECMS can achieve global optimal performance only when the overall driving velocity profile of the vehicle is known in advance. In this limited situation, the performance of the ECMS is almost identical to the global optimum using the DP [28]-[29].

Therefore, ECMS is a real-time implementation of PMP, and global optimal performance can be achieved if the driving profile of the future can be known in advance. However, since the driving velocity profile of the future can not be known in advance, adaptive ECMS (A-ECMS) that adaptively changes the control by utilizing only the current information has been studied. Research on A-ECMS using vehicle state information such as battery state of charge (SOC) has been conducted [28], [30]. In addition, a pattern recognition technique has been studied that derives a map of control through past accumulated data, recognizes the current driving pattern of the vehicle, and uses the control of the corresponding pattern from the map [31]-[33]. However, to realize the optimal performance of the ECMS, predicting the velocity profile is a more fundamental method. Although various studies have been carried out to predict the velocity profile of a vehicle directly using various prediction models, the reliability can be secured only for a very short time [34]-[37]. In the meantime, since it is difficult to predict driving information in the future with only the information inside the vehicle, researches have been conducted to utilize GPS, GIS, ITS, and other information gathered from outside the vehicle for ECMS control [38]-[40]. However, since information from outside the

vehicle is less reliable and resolution, research has been conducted through additional assumptions, and actual implementation at the current technology level is difficult.

1.3 Contributions

Contribution of this paper is the development of EMS using predictive-ECMS based on driving information. First, an environment was developed that enables forward simulation of vehicle performance through vehicle modeling and ECMS based EMS controller modeling. Secondly, various prediction models were developed to predict the control value of ECMS. These models use only driving information generated within the vehicle up to the present time as input data. Also, the prediction model directly predicts future ECMS control values as real values. Lastly, the prediction model was trained through past accumulated data. The performance of the predictive-ECMS controller, which combines the prediction model and the ECMS model, was evaluated through forward simulation.

The predictive-ECMS developed in this paper has the following differences compared to the previous studies. First, it is stand-alone EMS that do not use any information from outside the vehicle at all. Secondly, it is EMS that can realize real-time implementation at current technology level. Finally, performance close to optimal performance is realized while satisfying the above two conditions.

1.4 Thesis Outlines

The main body of this thesis composed of 5 chapters. Each chapter organizes as follows:

Chapter 2 describes the modeling and simulation environment of the vehicle. Modeling of powertrain component and vehicle architecture, and modeling of EMS based on ECMS. These models are combined to form a forward simulation environment.

Chapter 3 describes the development of prediction models. The method for obtaining the optimal control factor of the ECMS and the preprocessing of the historical cumulative data collected for the prediction model training are explained. Three different models of prediction were proposed using different techniques.

Chapter 4 describes the simulation analysis. This includes the comparison of the training results of three prediction models and the evaluation of the performance of the predictive-ECMS combined with the prediction model and ECMS.

Chapter 5 describes concluding remarks. Conclusion and future work of this thesis is presented.

Chapter 2. Vehicle Model Development

2.1 Target Vehicle

The target vehicle used in this study is a parallel type mild HEV. In addition to the configuration of conventional vehicle, this vehicle is a P0 type configuration in which the motor serving as an integrated starter-generator (ISG) is connected to the engine by a belt. Figure 2.1 shows the configuration of the target vehicle. It is a mild hybrid type with a maximum engine power of 134kW and a maximum motor power of 11kW. The motor is used only as a torque assist mode and regenerative power generation, and it is impossible to use the electric vehicle mode driven by the motor alone. Table 2.1 shows the target vehicle specifications. The powertrain component data was constructed with reference to the Autonomie vehicle system simulation tool of the Argonne National Laboratory.

Vehicle Parameters		Specification
Engine	Type	CI 4-Cylinder Diesel
	Maximum Power	134 kW
	Maximum Torque	392 Nm
Motor	Maximum Power	11 kW
	Maximum Torque	56 Nm
Battery	Capacity	10 Ah
Transmission	Type	6-Speed Automatic
Vehicle	Gross Weight	1495 kg
	Air Drag	0.35
	Frontal Area	2.61 m^2
Tire	Rolling Resistance	0.008
	Radius	0.34 m

Table 2.1 Target vehicle specification

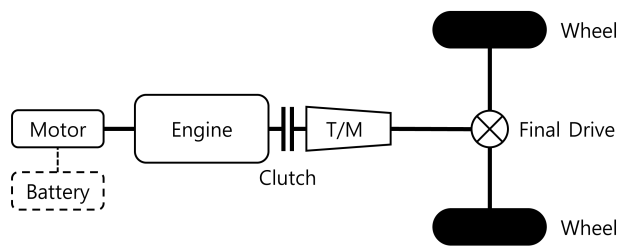

Figure 2.1 Target vehicle configuration

2.2 Vehicle Modeling

2.2.1 Engine Model

The engine used for the vehicle modeling is a four-cylinder diesel engine of compression ignition (CI) type. The maximum torque of the engine is 392Nm at 2500rpm and the maximum power is 134kW. The brake specific fuel consumption (BSFC) was modeled in the form of a map according to the engine torque and speed as expressed in (2.1). Therefore, the fuel consumption rate of the engine is expressed as a function of the engine torque and speed as shown in (2.2). Figure 2.2 shows the BSFC, maximum torque and optimal operating line (OOL) of the engine. The maximum efficiency range of the engine is located near the middle point of the operation speed and near the maximum load point.

$$\mathrm{BSFC} = function(T_{eng}, \omega_{eng}) \tag{2.1}$$

$$\begin{aligned} \dot{m}_{fc} &= \mathrm{BSFC} \times P_{eng} / (3600 \cdot 10^3) \\ &= \mathrm{BSFC} \times T_{eng}\omega_{eng} / (3600 \cdot 10^3) \\ &= function(T_{eng}, \omega_{eng}) \end{aligned} \tag{2.2}$$

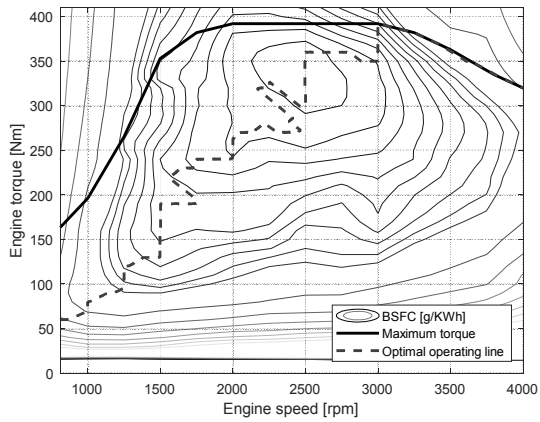

Figure 2.2 Engine BSFC map

2.2.2 Motor Model

The maximum torque of the motor used for the vehicle modeling is 56Nm at 1870rpm and the maximum power is 11kW. The efficiency of the motor was modeled in the form of a map according to the motor torque and speed as expressed in (2.3). Therefore, the power of the battery is expressed as a function of the motor torque and speed as shown in (2.4). Figure 2.3 shows the efficiency and maximum torque of the motor. The motor exhibits a large torque even in the stationary region and the low speed region, and the distribution of the maximum efficiency region is wider than that of the engine.

In the vehicle powertrain structure, the motor is connected to the engine by a belt with the speed coupling ratio $\gamma_{belt} = 2.5$ as shown in (2.5). Therefore, the required wheel torque of the vehicle can be expressed as (2.7).

$$\eta_{mot} = function(T_{mot}, \omega_{mot}) \tag{2.3}$$

$$P_{bat} = \eta_{mot} T_{mot} \omega_{mot} = function(T_{mot}, \omega_{mot}) \tag{2.4}$$

$$\omega_{mot} = \gamma_{belt} \omega_{eng} \tag{2.5}$$

$$P_{req} = P_{eng} + P_{mot} \tag{2.6}$$

$$\frac{T_{req,wheel}}{\gamma_{fd}\gamma_{gb}} \omega_{eng} = T_{eng}\omega_{eng} + T_{mot}\gamma_{belt}\omega_{eng} \tag{2.7}$$

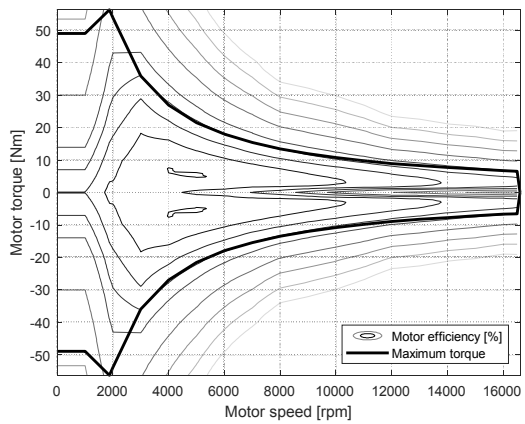

Figure 2.3 Motor efficiency map

2.2.3 Battery Model

The maximum capacity of the battery used for the vehicle modeling is 10Ah. The internal resistance model was used as the battery model, as shown in Figure 2.4. It is a model of the battery as a series connection of source voltage and internal resistance. The open-circuit voltage and internal resistance are functions of battery SOC and temperature, and the influence of temperature is neglected in this study as in (2.8). A graph of each function is shown in Figure 2.5. Using the battery internal resistance model, the SOC derivative of the battery can be calculated as shown in (2.11).

$$(V_{oc}, R_{int}) = function(\mathrm{SOC}) \tag{2.8}$$

$$R_{int} I^2 - V_{oc} I + P_{bat} = 0 \tag{2.9}$$

$$I = \frac{V_{oc} - \sqrt{V_{oc}^2 - 4R_{int}P_{bat}}}{2R_{int}} \tag{2.10}$$

$$\begin{aligned} \dot{\mathrm{SOC}} &= -\frac{1}{Q_{bat}} I \\ &= -\frac{1}{Q_{bat}} \frac{V_{oc} - \sqrt{V_{oc}^2 - 4R_{int}P_{bat}}}{2R_{int}} \\ &= function(\mathrm{SOC}, P_{bat}, Q_{bat}) \end{aligned} \tag{2.11}$$

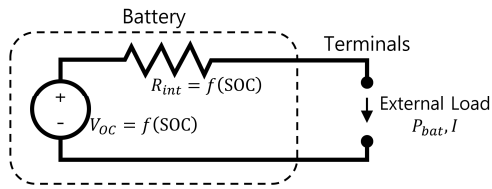

Figure 2.4 Battery internal resistance model

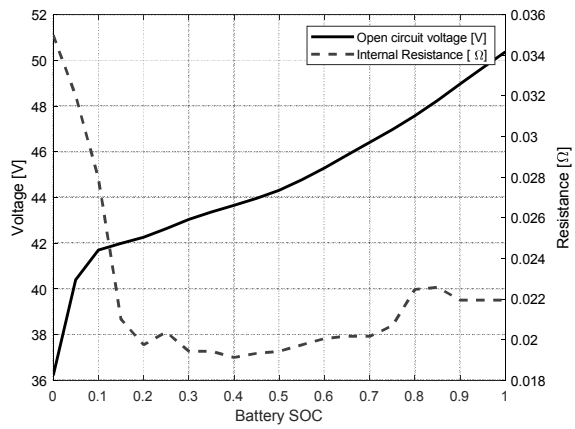

Figure 2.5 Battery specification map

2.2.4 Vehicle Model

The vehicle dynamics model used in this study only considers longitudinal dynamics, as shown in Figure 2.6. The dynamic equation of the vehicle is (2.12), and the resistance values considered in the model are rolling friction resistance (2.13), aerodynamic drag resistance (2.14), and gradient resistance (2.15). Finally, the vehicle model shown in Figure 2.7 is completed by combining the engine model, motor model, battery model and vehicle dynamics model, as well as the transmission model, other accessories and final reduction gear.

$$M\frac{dV}{dt} = \left(F_{tf} + F_{tr}\right) - \left(F_{rf} + F_{rr} + F_w + F_g\right) \tag{2.12}$$

$$\begin{aligned} F_r &= Wf_r = Mg\cos\alpha f_r \\ &= Mg\cos\alpha\left(f_0 + f_s\left(\frac{V}{100}\right)^{2.5}\right) \end{aligned} \tag{2.13}$$

$$F_w = \frac{1}{2}\rho A_f C_D\left(V + V_w\right)^2 \tag{2.14}$$

$$F_g = Mg\sin\alpha \tag{2.15}$$

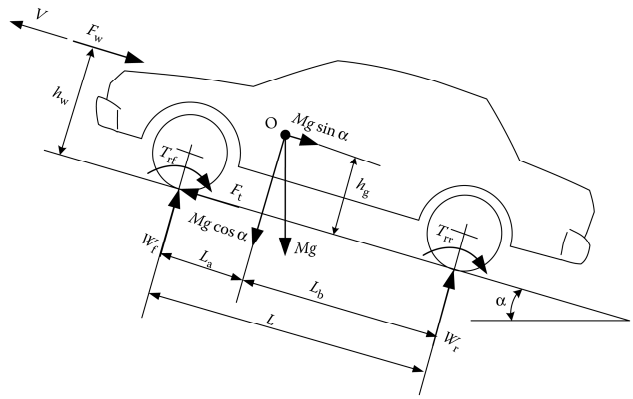

Figure 2.6 Longitudinal dynamics of vehicle

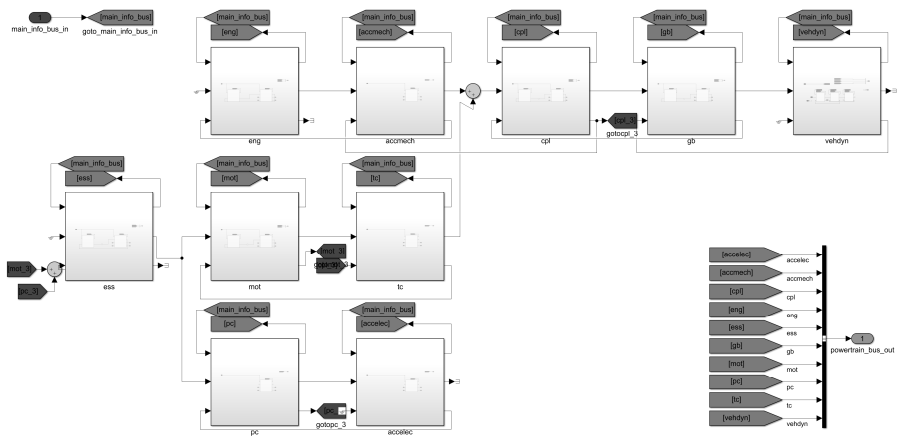

Figure 2.7 Vehicle modeling

2.3 Energy Management Strategy

HEVs have the engine and motor as power sources, and they have very different characteristics. In addition, HEVs made up of a variety of subsystems with the addition of the motor, inverter and battery in addition to the conventional powertrain subsystems. Therefore, in order to efficiently control the HEV, it is necessary to consider the advantages and disadvantages of the engine and the motor, and to distribute the power and to integrally control the subsystems.

2.3.1 Rule-Based Strategy

The most basic EMS of HEV is rule-based strategy. A rule-based strategy consists of several state and transition rules between states, and pre-defined control logic for each state. Since the vehicle model used in this study has no motor alone mode, in most cases the engine is on and limited off by parameters such as required wheel torque. The transition rule for engine on-off is shown in Table 2.2. There are three modes for distribution the required power to the engine and motor. The transition and control rule for each state is shown in the Table 2.3.

State	Transition
Engine Off	$T_{req,wheel} < -20\mathrm{Nm}$ (more than 0.1s) and $V_{veh} < 0.1\,\mathrm{m/s}$ and $\mathrm{SOC} > 0.45$ and $\mathrm{APS} < 0.8$
Engine On	else

Table 2.2 Transition rule for engine on-off

State	Transition / Control
Assist Mode	$T_{req,wheel} > 0$ and $\mathrm{SOC} > 0.6 \times 1.01$
	$T_{mot} = \frac{T_{req,wheel}}{\gamma_{fd}\gamma_{gb}}\left(1 + 0.4\left(V_{assist,\max}(\mathrm{SOC}) - V\right)\right) - T_{eng,\max}$
	$T_{eng} = \frac{T_{req,wheel}}{\gamma_{fd}\gamma_{gb}} - T_{mot}\gamma_{belt}$
Charge Mode	$T_{req,wheel} > 0$ and $\mathrm{SOC} < 0.6 \times 0.99$
	$T_{mot} = \frac{P_{bat,charge}(\mathrm{SOC}) - P_{acc,elec}}{\omega_{mot}}$
	$T_{eng} = \frac{T_{req,wheel}}{\gamma_{fd}\gamma_{gb}} - T_{mot}\gamma_{belt}$
Brake Mode	$T_{req,wheel} < 0$
	$T_{mot} = 0$
	$T_{eng} = \min\left(T_{eng,\max}, T_{eng,\min} + T_{acc,mech}(\omega_{eng})\right)$

Table 2.3 Transition and control rule for each power distribution mode

2.3.2 Equivalent Consumption Minimization Strategy

The EMS used in this study is developed based on ECMS. The ECMS is a control strategy that uses the total equivalent consumption energy as a cost function. The energy consumption rate of fuel and battery are as shown in (2.16) and (2.17). Equivalent to the energy consumption rate of the battery with the proportional constant, the total equivalent consumption energy is calculated as (2.18).

$$P_{fuel} = \dot{m}_{fc} \bullet LHV \tag{2.16}$$

$$\begin{aligned} P_{bat} &= V \bullet I \\ &= VQ_{bat}\dot{\mathrm{SOC}} \end{aligned} \tag{2.17}$$

$$\dot{m}_{eq} = \dot{m}_{fc} + k\frac{VQ_{bat}}{LHV}\dot{\mathrm{SOC}} \tag{2.18}$$

The voltage of the battery was constantly treated, and the equivalent factor is expressed in λ. The final cost function of the ECMS is shown in (2.19). The main advantage of ECMS is that it reduces global optimization problem to an instantaneous optimization criterion, with a cost function dependent only on the system parameters at the current time.

$$\begin{aligned} J &= \dot{m}_{eq} \\ &= \dot{m}_{fc} + \lambda\dot{\mathrm{SOC}} \end{aligned} \tag{2.19}$$

$$[T_{eng}, T_{mot}] = \mathrm{argmin}(J) \tag{2.20}$$

$$subject\ to \begin{cases} \mathrm{SOC}(t_0) = \mathrm{SOC}(t_f) \\ \mathrm{SOC}_{\min} < \mathrm{SOC} < \mathrm{SOC}_{\max} \\ T_{eng,\min} < T_{eng} < T_{eng,\max} \\ T_{mot,\min} < T_{mot} < T_{mot,\max} \end{cases}$$

2.3.3 Implementation of ECMS

The model of the ECMS controller was implemented as follows. When the required wheel torque $T_{req,wheel}$ of next time step $(t+1)$ is given from the driver, the torque of the engine and motor is distributed based on the vehicle parameters at the current time step (t) as follows. First, considering the specification of the motor, the candidate group of the motor power P_{mot} at the next time step $(t+1)$ is set as a vector of 1kW interval

from –11kW to 11kW. Considering (2.5) and (2.7), the candidate torque of the engine and motor are as follows.

$$T_{mot}(t+1)=\frac{P_{mot}(t+1)}{\gamma_{belt}\omega_{eng}(t)} \tag{2.21}$$

$$T_{eng}(t+1)=\frac{T_{req,wheel}(t+1)}{\gamma_{fd}\gamma_{gb}(t)}-\frac{P_{mot}(t+1)}{\omega_{eng}(t)} \tag{2.22}$$

Next, considering (2.11), (2.4) and (2.2), the candidates for SOC derivative and fuel consumption rate are as follows.

$$\begin{aligned}\dot{\mathrm{SOC}}(t+1)&=function\left(\mathrm{SOC}(t),P_{bat}(t+1),Q_{bat}\right)\\&=function\left(\mathrm{SOC}(t),T_{mot}(t+1),\gamma_{belt}\omega_{eng}(t),Q_{bat}\right)\end{aligned} \tag{2.23}$$

$$\dot{m}_{fc}(t+1)=function\left(T_{eng}(t+1),\omega_{eng}(t)\right) \tag{2.24}$$

Finally, considering (2.21) to (2.24), the cost candidate values of ECMS can be calculated, and the engine and motor torque that minimize the cost value are used as the torque of the next time step $(t+1)$. Modeling the control implementation of ECMS using MATLAB Simulink is shown in Figure 2.8.

$$\begin{aligned}J(t+1)&=\dot{m}_{fc}(t+1)+\lambda\dot{\mathrm{SOC}}(t+1)\\&=funtion\left(\lambda,T_{req,wheel}(t+1),P_{mot}(t+1),current\,states\right)\end{aligned} \tag{2.25}$$

$$\left[T_{eng}(t+1),T_{mot}(t+1)\right]=\mathrm{argmin}(J(t+1)) \tag{2.26}$$

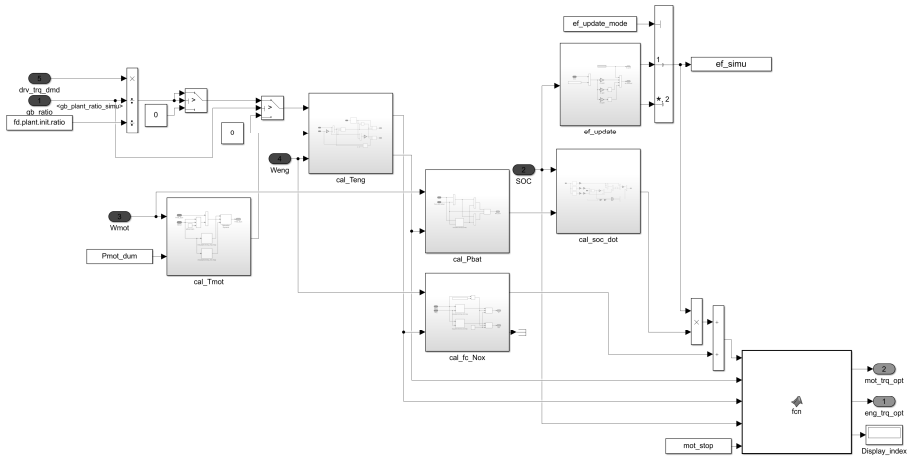

Figure 2.8 ECMS control modeling

2.4 Forward Simulation Environment

In this study, the forward simulation method was applied to simulate the fuel consumption of the vehicle. Generally, the fuel efficiency of a vehicle is evaluated by running a predetermined test cycle velocity profile. The forward simulation method has a virtual driver model. The driver model compares the test cycle with the current vehicle velocity and manipulates the accelerator pedal and the brake pedal to follow the test cycle velocity. The supervisory controller model distributes the power appropriately based on pedal signal using the EMS, and the vehicle model simulates the powertrain and dynamics of the vehicle based on control commands. As a result, this forward simulation method is an effective way to simulate the actual vehicle driving through the driver model. Figure 2.9 shows the configuration of the forward simulation environment based on the controller model and vehicle model.

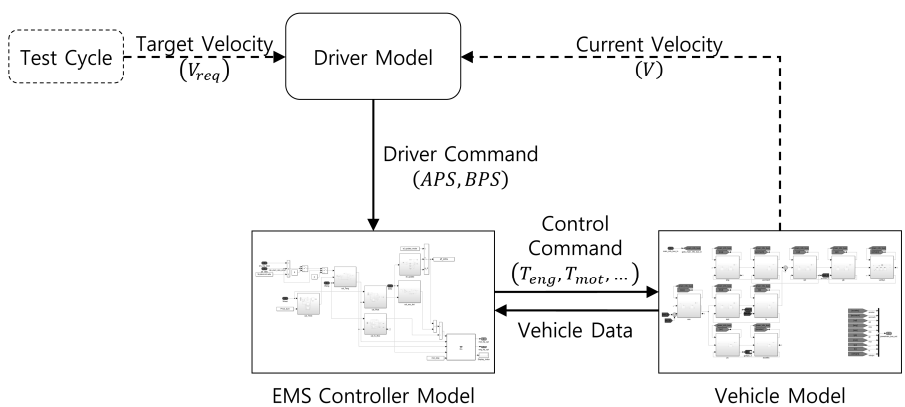

Figure 2.9 Forward simulation environment

Chapter 3. Prediction Model Development

3.1 Problem Definition

3.1.1 Optimal Equivalent Factor

In the ECMS control mentioned above, the equivalent factor of equalizing the energy consumption of the engine and the battery is the most important value. The ECMS control shows a large difference in the fuel consumption performance and the SOC sustaining performance depending on the equivalent factor. If the velocity profile of the vehicle is known in advance, an optimal value of the equivalent factor corresponding to the velocity profile can be obtained by iteration of the forward simulation. Figure 3.1 shows the simulation results of various equivalent factor for the WLTC cycle. The SOC trajectory was highly dependent on the equivalent factor. The SOC was sustained only when the optimal equivalent factor was used, and the vehicle achieve optimal performance.

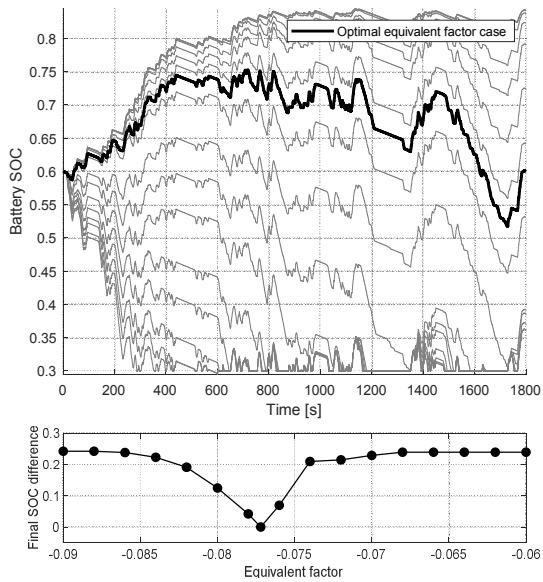

Figure 3.1 SOC trajectory according to the equivalent factor

To find out the potential maximum performance of the ECMS, the optimal equivalent factor for each fuel consumption measurement cycle was obtained. The optimal equivalent factor was obtained by iteration of forward simulation and iteration was performed until the difference between the final SOC and the initial SOC reached ± 0.0001.

The simulation using the existing rule-based control strategy was simulated as a comparative group. Since the final SOC may be different from the initial SOC when the rule-based control strategy is applied, the equivalent energy consumption E_{sum} was calculated for the performance comparison of the two control strategies. Equivalent energy consumption $E_{sum}$is calculated as (3.1).

$$\begin{aligned} E_{sum} &= E_{fuel} + E_{bat,dis} - E_{bat,char} \\ &= \left(LHV \int_{t_0}^{t_f} \dot{m}_{fc} dt + \int_{t_0}^{t_f} V_{dis} I_{dis} dt - \int_{t_0}^{t_f} V_{char} I_{char} dt \right) / \left(3600 \cdot 10^3 \right) \end{aligned} \tag{3.1}$$

The simulation results for the equivalent energy consumption E_{sum} and SOC difference SOC_{delta} for both control strategies are shown in Table 3.1, and the relative E_{sum} value of the optimal ECMS case for rule-based of each cycle is shown in Figure 3.2. The optimal ECMS consumed an average of 10.31kWh of energy and 10.50kWh in the case of rule-based strategy. The energy consumption of the two strategies showed an average difference of 2.549% and maximum 5.556% for each cycle.

	Optimal ECMS	Rule-based	
	E_{sum} [kWh]	E_{sum} [kWh]	SOC_{delta}
EUDC	3.451	3.565	0.096
HWFET	7.236	7.279	0.039
Inrets Highway	29.46	29.70	0.034
Inrets Road	6.497	6.720	0.026
NEDC	5.474	5.796	0.096
UDDS	6.394	6.569	0.002
WLTC	13.65	13.89	0.064
Average	10.31	10.50	0.051

Table 3.1 Performance comparison
between optimal ECMS and rule-based strategy

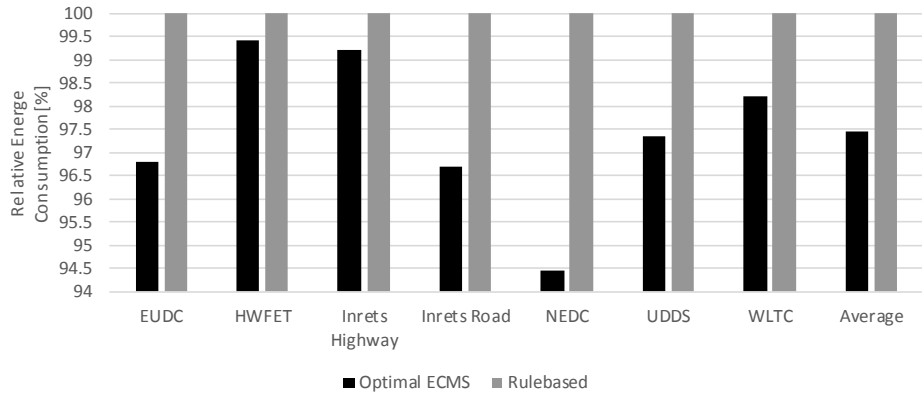

Figure 3.2 Energy consumption comparison between optimal ECMS and rule-based strategy

3.1.2 Periodic Application of Optimal Equivalent Factor

On the other hand, since the optimal equivalent factor of ECMS is dependent on the velocity profile, the potential maximum performance of ECMS can be realized only if entire future driving cycle is known in advance. However, in the actual situation, the optimal equivalent factor can not be known because the future driving cycle is not known. Therefore, the equivalent factor should be predicted through an appropriate prediction model. The global optimal equivalent factor for entire future driving cycle is very difficult to predict because it is dependent on the entire future driving cycle.

Therefore, in this study, a method of predicting the optimal equivalent factor periodically with a certain time window length is proposed. It is very important to select the appropriate window size in this method. The larger window size, the closer to the globally optimized energy consumption, but the predictability of equivalent factor becomes more difficult because the equivalent factor depends on the information of a far future. The smaller window size, the easier it is to predict the equivalent

factor, but the energy consumption is no different from the rule-based strategy. Therefore, an appropriate window size should be selected to achieve a performance similar to the globally optimized energy consumption performance with a suitably short window size.

If the driving cycle is equally divided according to the window size, each micro trip becomes a short driving cycle with the non-zero initial velocity. Forward simulation is generally difficult to simulate in such a micro trip, so the following method was used to find the optimal equivalent factor for a short driving cycle that does not start from a stop state.

In order to start from the stop state, the stop section, the constant acceleration section and the constant velocity section were added at the front of the micro trip for 10 seconds each. The iterative simulation was performed by changing the initial SOC SOC_{init} and equivalent factor λ for modified micro trip, and the iteration was repeated until the difference between the SOC at the time of 30 seconds and the final SOC is within $\pm$ 0.001. The pseudo-code for the process of obtaining the optimal equivalent factor through iteration is shown in Figure 3.3.

iteration for SOC_{init}

  iteration for λ

    run forward simulator with (SOC_{init}, λ)

    $SOC_{mid,\,delta} = SOC_{mid} - SOC_{mid,target}$

    $SOC_{fin,\,delta} = SOC_{fin} - SOC_{fin,target}$

    $SOC_{rel,\,delta} = SOC_{fin,delta} - SOC_{mid,delta}$

    if $SOC_{rel,\,delta} > 0.001$

      $$\lambda = (1-0.2)\left(\frac{SOC_{fin,\,delta}}{SOC_{fin}}\right)^2 \lambda$$

    else if $SOC_{rel,\,delta} < 0.001$

      $$\lambda = (1+0.2)\left(\frac{SOC_{fin,\,delta}}{SOC_{fin}}\right)^2 \lambda$$

    else

      break

  end

  if $|SOC_{rel,\,delta}| < 0.001$ & $|SOC_{mid,\,delta}| < 0.001$

    break

  else

    $SOC_{init} = SOC_{init} - SOC_{mid,delta}$

end

Figure 3.3 Pseudo code for obtaining optimal equivalent factor

The example of changing the equivalent factor and relative SOC difference $SOC_{rel,\,delta}$ during the iteration process is shown in Figure 3.4. In general, these two variables have a s-curve like the dotted line. Figure 3.5 shows the variation of the SOC trajectory in the iteration process.

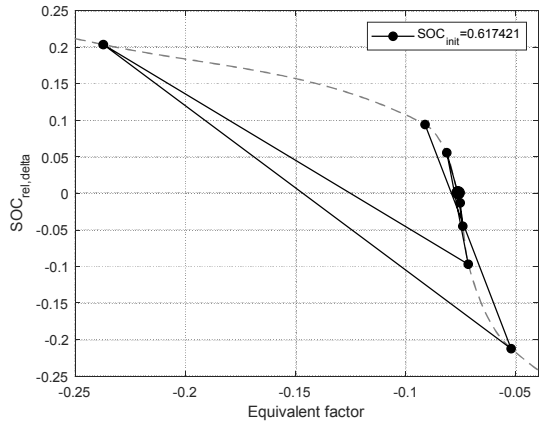

Figure 3.4 Equivalent factor and relative SOC difference during iteration

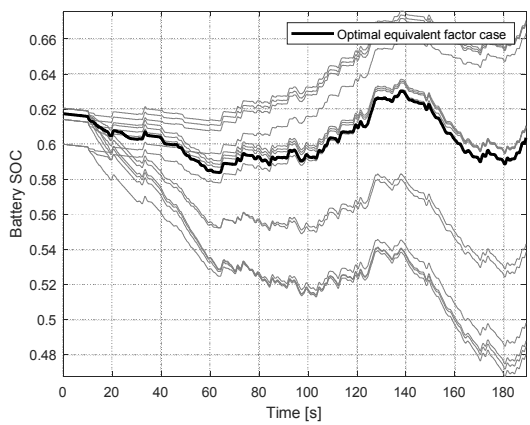

Figure 3.5 SOC trajectory during iteration

By applying this iteration method, the optimal equivalent factor for micro trip can be obtained, and iterative simulation was performed on various window sizes to find an appropriate window size. The case of using equivalent factor based on divided cycle with specific window size, the case of using global optimal equivalent factor and the case of using the rule-based strategy were compared. The window size was set to 20 to 320 seconds divided by 20 seconds. Equivalent energy consumption E_{sum} was

calculated for the performance comparison and the relative value for energy consumption of optimal ECMS case was used.

The simulated average values for each of the 10 driving cycles are shown in Table 3.1 and Figure 3.6. As expected, the shorter the window size, the more energy was consumed and increased to a similar value to the case of rule-based. Also, as the window size increases, the energy consumption decreased to a value similar to that of the optimal ECMS case. It can be seen that the decreases of the energy consumption due to the increase of the window size was almost converged when the window size was 160 seconds. When the window size was 160 seconds, the energy consumption was only 0.316% difference from the optimal ECMS. Based on these results, the rest of the study is conducted with a window size of 160 seconds.

Window size [s]	E_{sum} [kWh]	Window size [s]	E_{sum} [kWh]
(Optimal ECMS)	10.3095	160	10.3325
320	10.3197	140	10.3389
300	10.3280	120	10.3287
280	10.3268	100	10.3377
260	10.3208	80	10.3426
240	10.3173	60	10.3478
220	10.3296	40	10.3584
200	10.3253	20	10.4062
180	10.3288	(Rule-based)	10.5027

Table 3.2 Energy consumption comparison according to window size (Average value of 7 cycles)

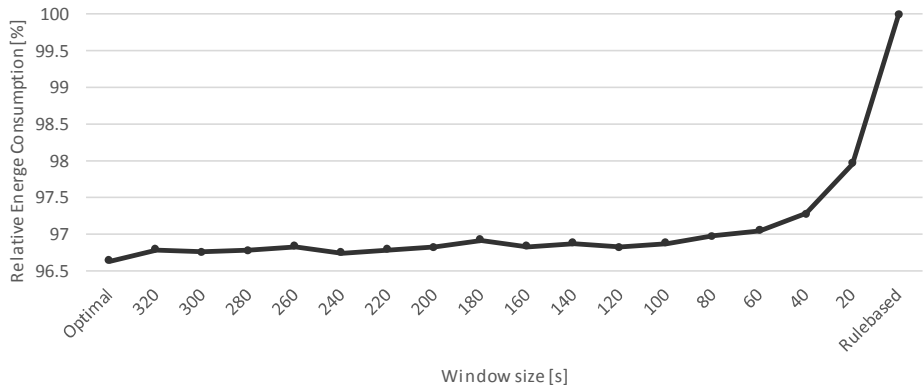

Figure 3.6 Energy consumption comparison according to window size

3.1.3 Training Data Preprocessing

A training data set is needed to train the prediction model that predicts the optimal equivalent factor. The data for training was collected. Among the publicly known fuel efficiency measurement cycles widely used in the world, the cycle suitable for passenger sedans was used as the data for training. The collected driving cycle was 97,946 seconds, which was divided into 160 seconds to construct a micro trip. In addition, since the number of training data sets is insufficient, the training data was augmented by shifting the whole driving cycle. The data augmentation was carried out 30 times, resulting in a total of 18,363 micro trips. The collected driving cycles and data augmentation process are shown in Figure 3.7. For each of these micro trips, the optimal equivalent factor of individual micro trips were calculated in advance by the iteration method described above. The standard deviation of the obtained optimal equivalent factor was 0.00710.

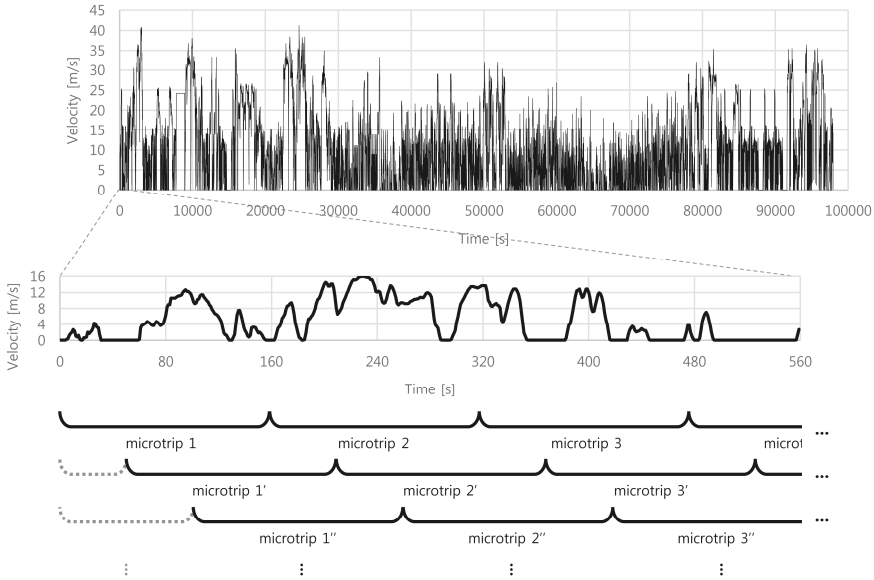

Figure 3.7 Collected data and augmentation process

3.2 Prediction Model based on Driving Information

3.2.1 LSTM Model using Time Series Data

Various studies have been carried out to predict the future driving environment, but most of them have been predicted through additional information from the outside of the vehicle. In particular, there are a number of studies conducted on the assumption that vehicle know information that can not be obtained at the present level of technology. However, these prediction models have a fatal drawback that they are overly dependent on traffic information systems and can not operate offline. The prediction model proposed in this study uses only the information obtained from the vehicle.

The driving data generated by the vehicle are basically time series data. A suitable model for this time series data processing is a recurrent neural network (RNN) model. Among the deep learning supervised models, the RNN model shows great performance in time series data processing. In general, sigmoid function and hyperbolic tangent function are used as the activation function of the RNN. However, in the case of these RNN cell, there is a limitation in expressing the dependency over time of the time series data due to the gradient vanishing problem or the gradient exploding problem in the back propagation process over time.

As a solution to this problem, a long short-term memory (LSTM) cell which extends an existing RNN cell has been introduced. The LSTM cell shows high performance over long time dependency using input gate, forget gate, memory cell and output gate. A total of four gates and memory cells each are a kind of feed forward network, each having a weight and bias. The LSTM learning process consists of training these weight and bias

through back propagation. The operation formulas for output values in each gate and cell in one LSTM cell unit are as follows, and the form of the cell in LSTM unit and total LSTM model structure is shown in Figure 3.8.

$$i_t = \sigma(w_i \bullet [h_{t-1}, x_t] + b_i) \ : \text{ input gate} \tag{3.2}$$

$$\tilde{c}_t = \tanh(w_c \bullet [h_{t-1}, x_t] + b_c) \ : \text{ input gate} \tag{3.3}$$

$$f_t = \sigma(w_f \bullet [h_{t-1}, x_t] + b_f) \ : \text{ forget gate} \tag{3.4}$$

$$o_t = \sigma(w_o \bullet [h_{t-1}, x_t] + b_o) \ : \text{ output gate} \tag{3.5}$$

$$c_t = f_t \circ c_{t-1} + i_t \circ \tilde{c}_t \ : \text{ update cell state} \tag{3.6}$$

$$y_t = h_t = o_t \circ \tanh(c_t) \ : \text{ update hidden state} \tag{3.7}$$

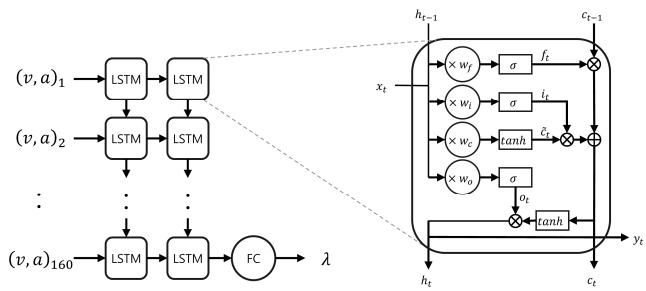

Figure 3.8 LSTM unit cell and model structure

For the training data of the LSTM model, the velocity and acceleration time series data for 160 seconds at 1 second interval were used, and the target data was the optimal equivalent factor for the next time window 160 seconds later. The LSTM model consisted of two LSTM layers, the dimension of the cell state and hidden state of the first layer was set to 128 and the second layer was 64. The output value from the last cell of the second layer passes through the fully connected layer and becomes the final output.

3.2.2 MLP Model using Feature Data

In the case of the above-mentioned LSTM model, the prediction model was trained only by the raw data of the driving information including the vehicle velocity and the acceleration. In general, however, feature values such as average velocity or average acceleration are used for driving information analysis rather than raw data. The LSTM model only allows the model to find the most relevant value among the various features by inputting the raw data intact. Therefore, it is necessary to extract the features manually from the raw data, and to train the prediction model with these features.

Generally, multi-layer perceptron (MLP) models have shown high performance in this training. The perceptron is an artificial neuron and it has a structure that multiplies the input values by weight and then combines all with bias to pass a specific activation function. The MLP model is a kind of feed forward network in which these perceptrons are arranged in parallel and stacked in layers. The structure of the MLP model is shown in Figure 3.9.

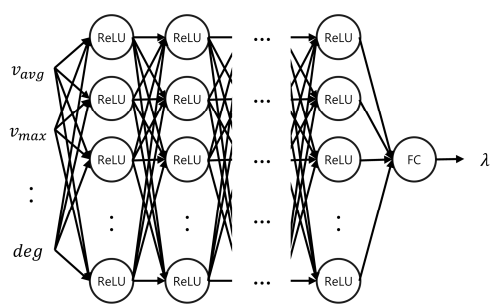

Figure 3.9 MLP model structure

As the training data of the MLP model, nine features extracted

from the 160 second driving data were used, and the target data was the optimal equivalent factor of the next time window. The nine features are the distance, average velocity, maximum velocity, average acceleration, maximum acceleration, average deceleration, maximum deceleration, aggressiveness and degressiveness for 160 seconds respectively. Each layer of the MLP model consisted of 100 perceptron respectively and 10 layers were stacked. The rectified linear unit (ReLU) was used as the activation function. The output values of the last layer pass through the fully connected layer and become the final output.

3.2.3 LSTM-MLP Model using Multiple Data

The two proposed prediction models use raw driving information and manually extracted features as input data respectively. Since these input data have their own advantages, a multiple input prediction model using both input data is proposed. In this specially designed prediction model, the output of the LSTM model is transferred through a fully connected layer to an input of the MLP model. This means that the output value of the LSTM model is used as the tenth feature in the MLP structure. Figure 3.10 shows the structure of the merged LSTM-MLP model. The training data of the LSTM-MLP model used 160 seconds of time series data and nine extracted features from time series data as multiple inputs. The target data was likewise the optimal equivalent factor of the next time window.

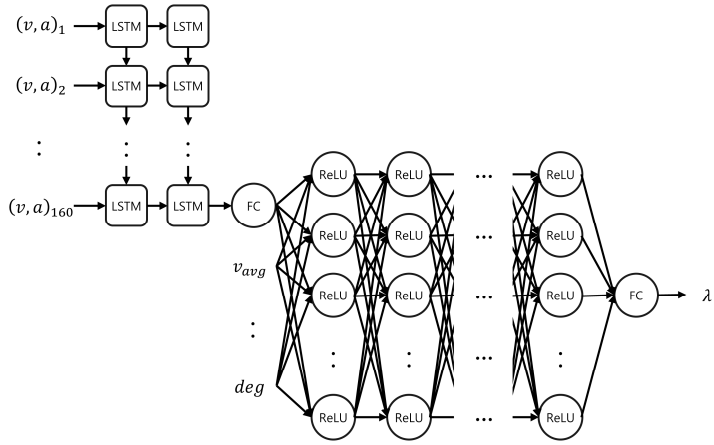

Figure 3.10 LSTM-MLP model structure

Chapter 4. Simulation Analysis

4.1 Prediction Model Training

The data used for the training of the prediction model was 18,363 dataset mentioned above. Each dataset consisted of 160 seconds of driving information as input data, and the optimal equivalent factor for the next 160 seconds obtained by iteration as the target data. The driving information means the velocity and acceleration time series data for 160 seconds and the nine features extracted from it. The time series dana and features used as input data were standardized with their respective mean and standard deviation. Only 80% of the data were used for training, 10% for validation and the remaining 10% for testing. The prediction model was constructed using python TensorFlow.

4.1.1 LSTM Model using Time Series Data

The LSTM Model used only time series data as input data as mentioned in the previous chapter. The predicted results of the equivalent factor and the correct answer value for a test set are shown in Figure 4.1. The average of the distribution was similar, but the precision was somewhat lower, and in particular, the region where the low value was the target was not predicted at all. This is because the feature was not manually extracted and used as input data, but only time series data was used as raw data. In other words, the LSTM model alone can not detect the high level feature that is related to the optimal equivalent factor of the future. The distribution of the predicted and target values is shown in Figure 4.2, the root mean

squared error (RMSE) was 0.00406 and correlation coefficient was 0.665.

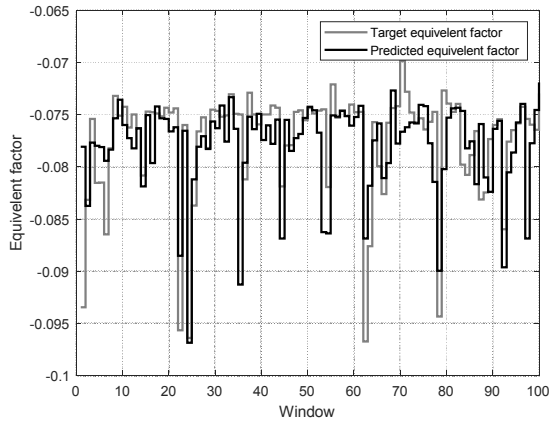

Figure 4.1 LSTM model test result

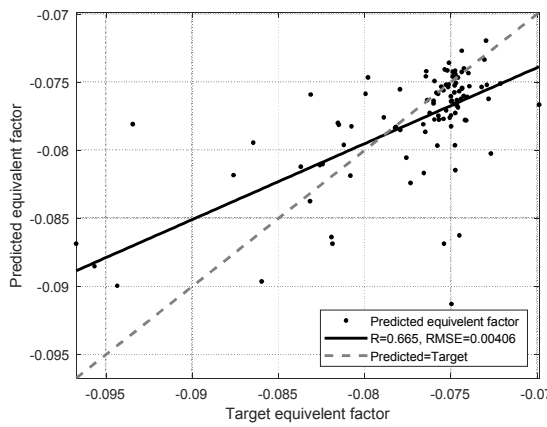

Figure 4.2 LSTM model test result

4.1.2 MLP Model using Feature Data

The MLP Model used only feature data as input data as mentioned in the previous chapter. The predicted results of the equivalent factor and the correct answer value for a test set are shown in Figure 4.3. The

accuracy of the predicted factor of the MLP model was much better than that of the LSTM model, and precisely predicted a region with a particularly low target value. This is probably due to the use of manually extracted feature data as input. The distribution of the predicted and target values is shown in Figure 4.4, the RMSE was reduced to 0.00376 and correlation coefficient was 0.751.

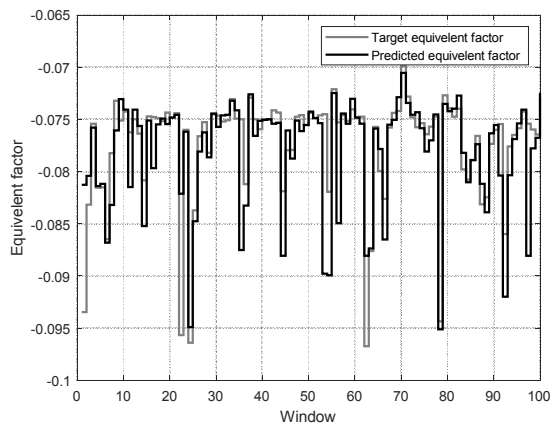

Figure 4.3 MLP model test result

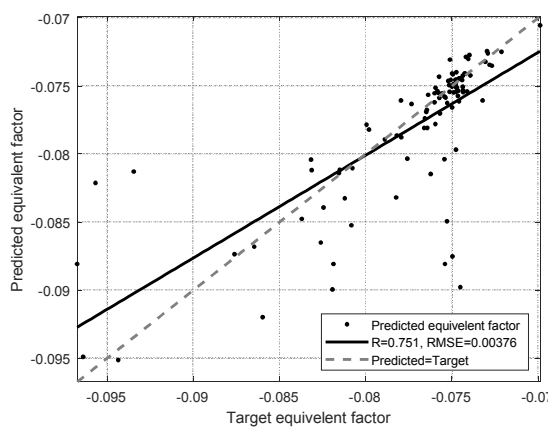

Figure 4.4 MLP model test result

4.1.3 LSTM-MLP Model using Multiple Data

The LSTM-MLP model used both time series data and feature data as input data. The predicted results of the equivalent factor and the correct answer value for a test set are shown in Figure 4.5. The prediction accuracy in the section with a small equivalent factor value was relatively accurate and the prediction accuracy around –0.075, which is a factor value mainly, was much higher than the MLP model. It can be seen that the prediction error was much lower when the two models were used in combination as compared with when the LSTM model or the MLP model alone was used. The distribution of the predicted and target values is shown in Figure 4.6, the RMSE was reduced to 0.00308 and correlation coefficient was 0.829. Figure 4.7 shows the decrease of the loss value in the training process of the LSTM-MLP model. The decrease trend of the loss for validation set was continuously monitored and training was terminated when the loss converged.

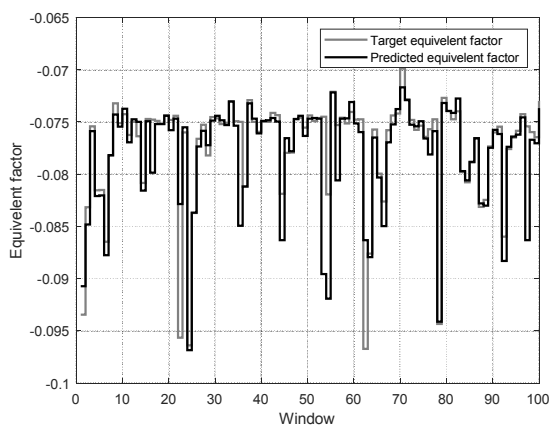

Figure 4.5 LSTM-MLP model test result

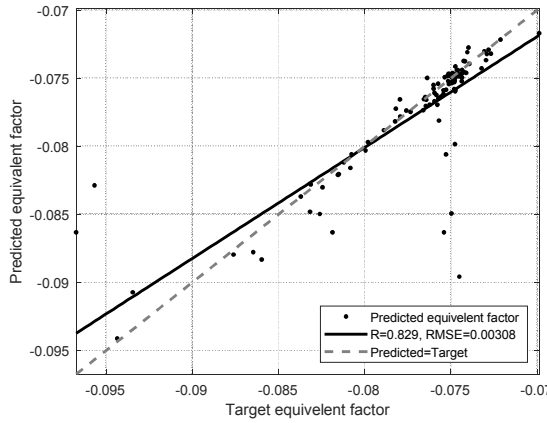

Figure 4.6 LSTM-MLP model test result

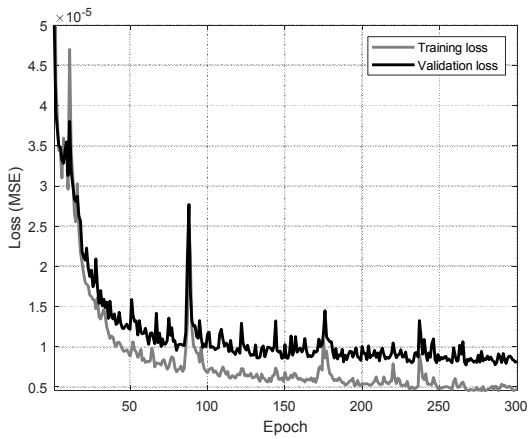

Figure 4.7 LSTM-MLP model training log

4.2 Vehicle Simulation using Energy Management Strategy based on Predictive ECMS

The schematic diagram of EMS using ECMS based on prediction model is shown in Figure 4.8. The control flow is divided into an offline calculation part outside the vehicle and an online calculation part of the vehicle in real-time control. In the offline calculation part, the historical cumulative driving data is used, and through the data preprocessing, the iteration of the equivalent factor optimizer finds the optimal factor and trained by the predictor. The trained predictor is transferred to the vehicle, which is used in online calculation section to control the vehicle based on the ECMS. Also, the driving data collected while driving are stored in the memory of the vehicle, and then transferred to offline calculator to be used for retraining the predictor.

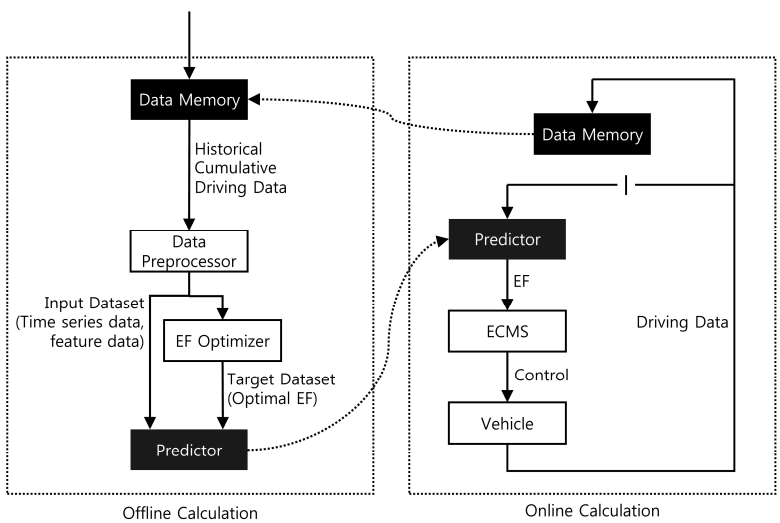

Figure 4.8 Control flow schematic diagram

The performance evaluation of the strategy was performed using the

forward simulation described above. The predictor was constructed using the LSTM-MLP model among the above three prediction models. In predictor, the equivalent factor for the first time window immediately after the departure without previous driving information was set to the average of the optimal factor used in the prediction model training. From the next time window, the predicted equivalent factor was used through the pre learned prediction model, using the driving information from the previous time window driving.

The results of the forward simulation of predictive-ECMS using the LSTM-MLP prediction model are summarized in Table 4.1. Equivalent energy consumption E_{sum} and SOC difference SOC_{delta} results were compared with optimal ECMS and rule-based cases, respectively. The relative E_{sum} value of the optimal ECMS case and predictive-ECMS for rule-based of each cycle is shown in Figure 4.9.

The predictive-ECMS consumed an average of 10.35kWh of energy, which is 2.01% less than the 10.50kWh of the rule-based case. The optimal ECMS consumed an average of 10.31 kWh of energy, which is 2.55% less than the rule-based case. In other words, predictive-ECMS showed 0.54%p difference compared to optimal case and showed almost close performance. This tendency was the same for all driving cycles used in the simulation.

Therefore, it can be said that the case of the predictive-ECMS using only the prediction model without knowing the future information was close to the case of the optimal ECMS assuming that the entire information is all known in advance. This suboptimal performance was also demonstrated reliably regardless of the driving cycle. Since the target vehicle was a mild HEV, the energy savings were not dramatic, but they were significantly more energy efficient than the well-tuned rule-based and were close to optimal case.

On the other hand, in case of SOC sustain performance, the variation of SOC was changed by 5.1%p on average compared to 60% of initial SOC at the beginning of driving in case of rule-based. However, in the case of predictive-ECMS, the variation of SOC was 3.9%p, which means that SOC was better maintained. In particular, SOC sustain performance of predictive-ECMS was always better than rule-based except for two driving cycles.

	Optimal ECMS	Predictive-ECMS		Rule-based	
	E_{sum} [kWh]	E_{sum} [kWh]	SOC_{delta}	E_{sum} [kWh]	SOC_{delta}
EUDC	3.451	3.487	0.046	3.565	0.096
HWFET	7.236	7.265	0.025	7.279	0.039
Inrets Highway	29.46	29.50	0.029	29.70	0.034
Inrets Road	6.497	6.526	0.008	6.720	0.026
NEDC	5.474	5.545	0.116	5.796	0.096
UDDS	6.394	6.403	0.007	6.569	0.002
WLTC	13.65	13.71	0.045	13.89	0.064
Average	10.31	10.35	0.039	10.50	0.051

Table 4.1 Performance comparison between optimal ECMS, predictive-ECMS and rule-based strategy

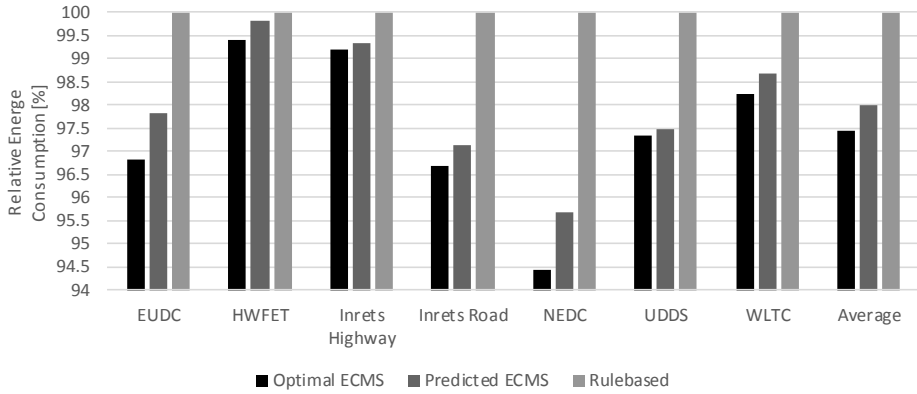

Figure 4.9 Energy consumption comparison between optimal ECMS, predictive-ECMS and rule-based strategy

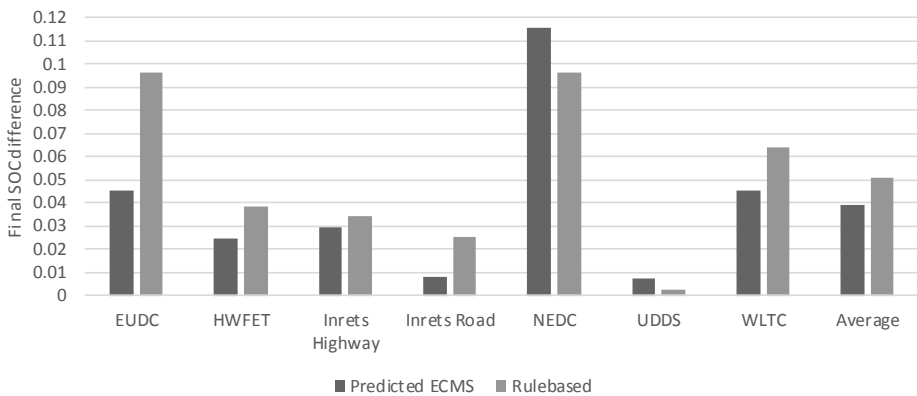

Figure 4.10 SOC sustain performance comparison between optimal ECMS, predictive-ECMS and rule-based strategy

Figure 4.11 is a graph comparing the simulation results for the Inrets Road cycle, which is a middle speed test cycle. The prediction of the equivalent factor through the prediction model predicted a value that almost matches the target value except for the first window and the last window. In the case of the first window, the error was generated because the data was not yet collected and the default value was output. In the case of the last window, it was an error that occurs because model did not know that

the driving will end in the middle of the window and factor was predicted for complete 160 seconds driving. Therefore, it can be said that the prediction accuracy was very high except for these two windows which can not be predicted correctly.

Comparing the SOC trajectory, the initial and final SOCs were fixed at the reference value of 60% in the case of the optimal ECMS, and the battery power was used in a very fluid manner. Predictive-ECMS tried to reach the SOC value to the reference value of 60% at each time window boundary, and the battery power was used fluidly within each window. Although the initial equivalent factor can not be predicted, and the SOC at the end of the first window was lower than reference value, but it tends to recover as time goes by. Also the SOC sustain result after the end of the driving of the predictive-ECMS case was better than rule-based case.

Overall, the predictive-ECMS did not use SOC as freely as the optimal ECMS, but it was relatively fluid rather than rule-based, resulting in a tendency to use the trajectory closer to optimal SOC trajectory than rule-based.

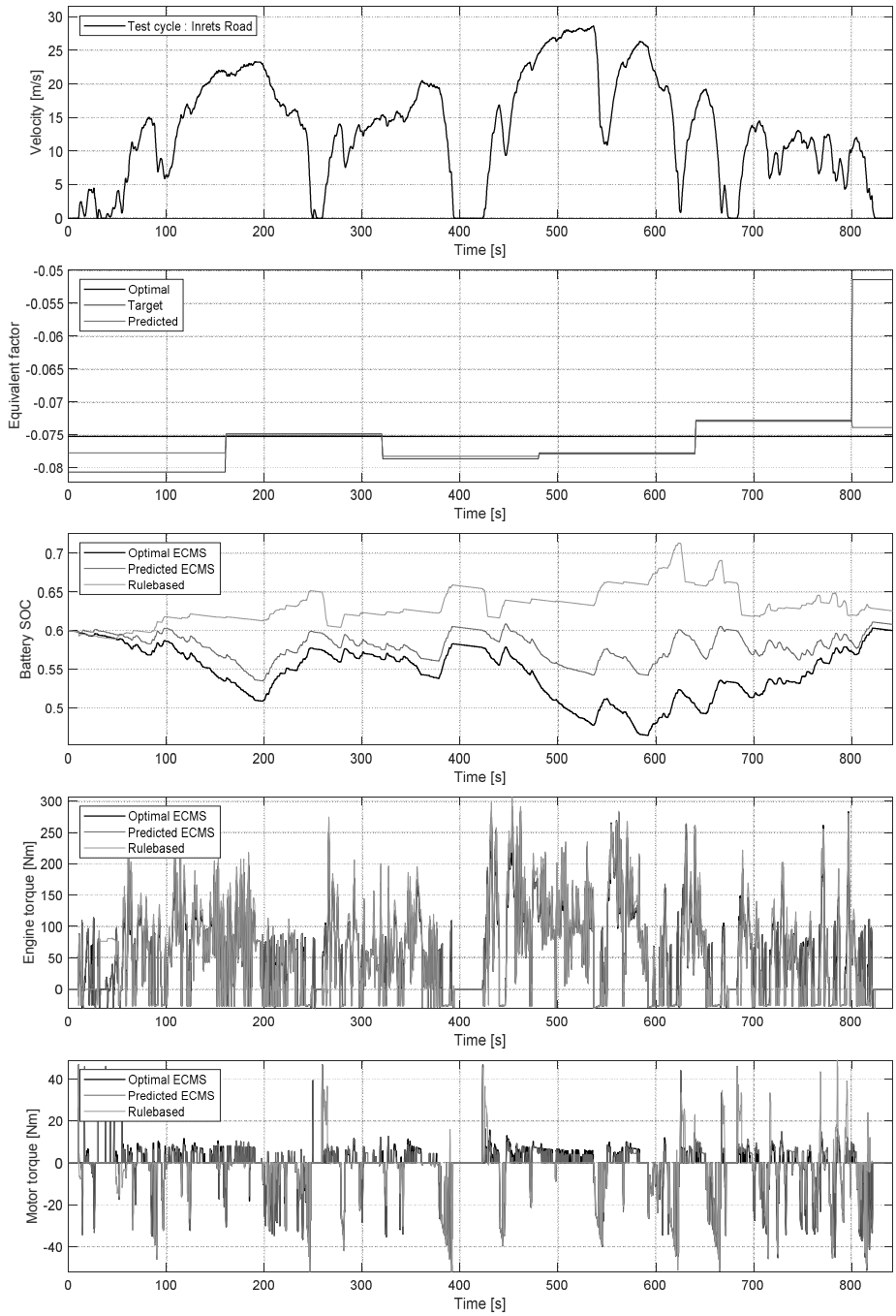

Figure 4.11 Simulation results of Inrets Road cycle

Figure 4.12 is a graph comparing the simulation results for the WLTC cycle, which is a combined test cycle of urban and high speed driving. As a result of the prediction of the equivalent factor through the prediction model, it can be seen that the predicted value was estimated similar to the target value except for the first window and the last window. Therefore, except for these two windows which can not be predicted, the prediction accuracy was relatively high.

Comparing the SOC trajectory, the optimal ECMS used the battery power very freely as a whole. The predictive-ECMS showed a tendency to reach the reference value for the period of the time window, but was relatively fluid. On the other hand, in the case of rule-based, it tried very strongly to maintain the reference value of 60%. Also the result of the SOC sustain after the end of the driving of predictive-ECMS was batter than that of rule-based case.

As a result, predictive-ECMS was less fluid than optimal ECMS, but more free than rule-based case in using SOC. In particular, the SOC trajectory of the predictive-ECMS showed a similar increase or decrease in the shape of the optimal ECMS trajectory as if it were reduced to the 60% baseline direction.

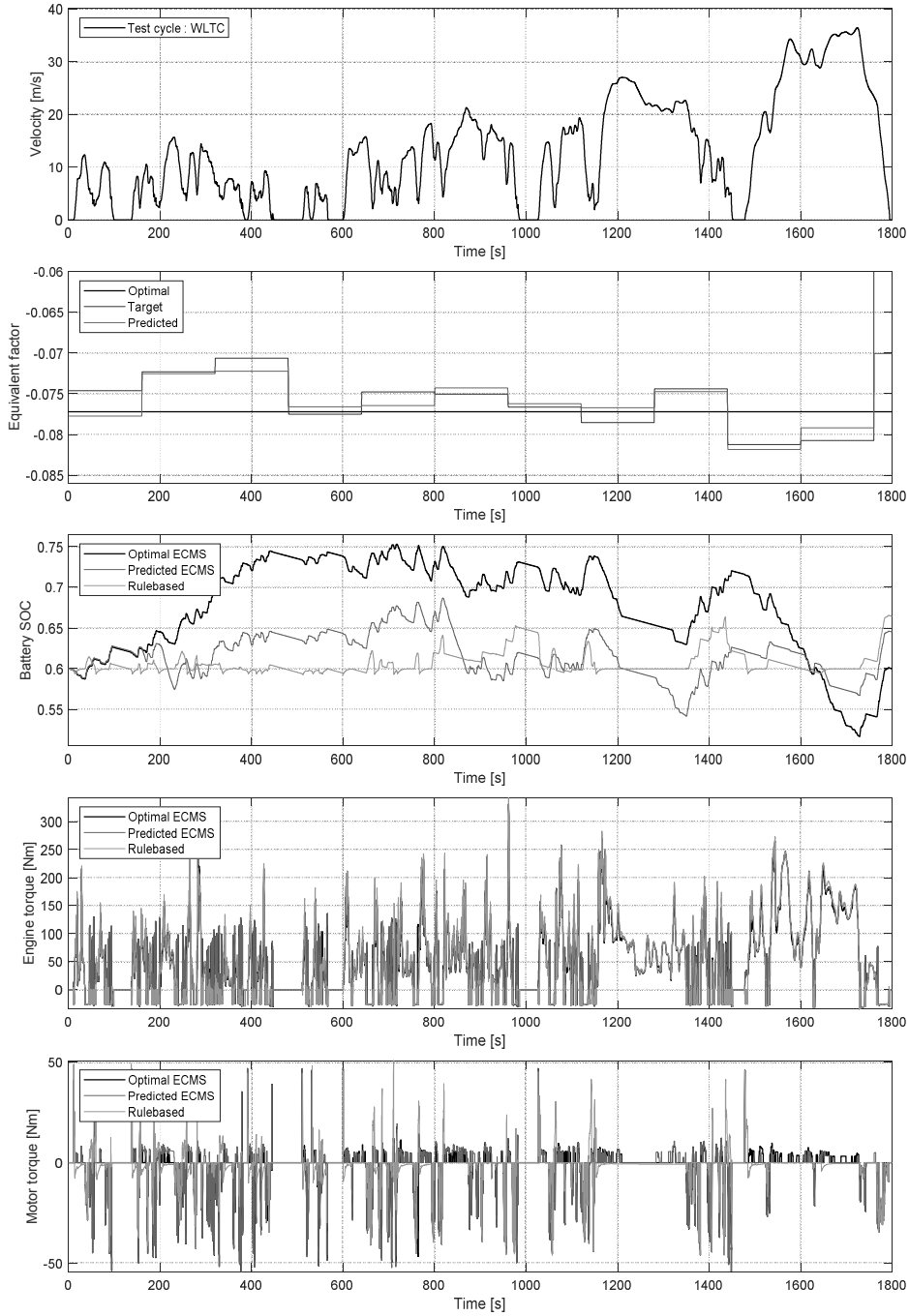

Figure 4.12 Simulation results of WLTC cycle

Figure 4.13 compares the simulation results for the Inrets Highway cycle, which is a high speed driving test cycle. The predicted result of the equivalent factor through the prediction model showed that the prediction of the target value was similar to that of the target value except for the first window and the last window. Therefore, except for these two windows which can not be predicted, the prediction accuracy was relatively high.

Comparing the SOC trajectory, the optimal ECMS used the battery power as a whole. Especially, it was shown that the motor was driven in the high speed travel region and the SOC was charged again in the acceleration and deceleration region at the end of the cycle. The predictive-ECMS showed a tendency to keep the SOC close to the reference value at high speed region. This was because it was not known in advance that SOC charging was possible in the acceleration and deceleration region at the end of the cycle. On the other hand, in the case of rule-based, the engine was used instead of the motor in the initial acceleration and deceleration section, and the surplus SOC was gradually decreased, resulting in a somewhat inefficient trajectory. Similarly, the SOC sustain result after the end of the driving was better than when the predictive-ECMS was rule-based.

As a result, due to the characteristics of high speed driving, the improvement of fuel efficiency was smaller than the urban driving, predictive-ECMS showed limited SOC usage than optimal ECMS, but still achieved better fuel economy than rule-based using inefficient SOC trajectory.

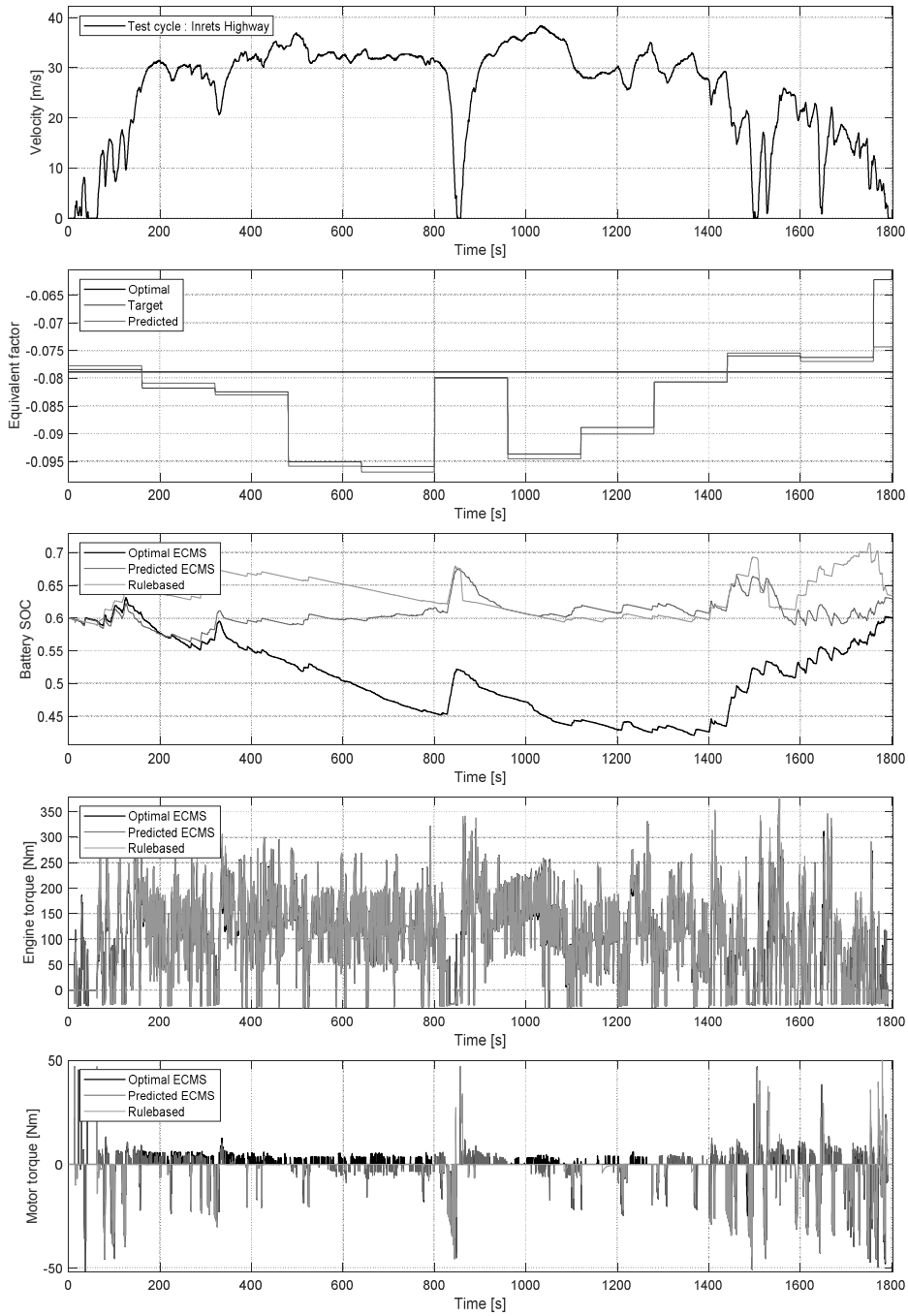

Figure 4.13 Simulation results of Inrets Highway cycle

Chapter 5. Conclusion

5.1 Conclusion

In this thesis, the predictive-ECMS EMS based on driving information for HEV was developed. For this, mild HEV and ECMS based EMS were modeled and three types of prediction model were developed. Driving information datasets for model training were collected and appropriately preprocessed. Training datasets were used to train each of the three prediction models and compared the test results. The predictive-ECMS using prediction model with the best prediction performance was simulated by HEV modeling and the results were analyzed.

The prediction performance of the LSTM model using time series data, which is raw data of driving information, was insufficient. However, MLP model using features that extracted manually from driving information had relatively good prediction performance. The LSTM-MLP model, in which one output of the LSTM model was added to MLP model as a new feature, increased prediction accuracy even further.

The forward simulation results of the predictive-ECMS EMS using the LSTM-MLP prediction model are as follows. Compared to optimal ECMS assuming that all future information is known in advance, the predictive-ECMS showed near energy usage. Compared with rule-based EMS applied to existing vehicles, much less energy was used. Also, the SOC sustain performance comparing the SOC at the beginning and the end of the driving was also better than the predictive-ECMS than the rule-based EMS. In particular, the above performance improvements were consistent for most test driving cycles.

The mild HEV that maximizes the fuel efficiency of conventional vehicles requires adequate EMS because of the relatively small battery and motor capacity. Rule-based EMS, which has been applied to existing vehicles, is not enough to draw the potential of mild HEVs. However, optimization based EMS is hard to implement because it requires future information. It is expected that commercialization of optimization based EMS will be made if research on EMS based on the prediction model like this thesis is continuously performed.

5.2 Future Work

This thesis proposed a supervisory EMS of a hybrid using a unique prediction model. There are some additional works that need to be addressed to improve the completeness of the proposed EMS.

First, it is necessary to verify the robustness of the prediction model. In this study, only stable conditions were verified rather than actual driving conditions. The battery SOC was operated only within a reasonable range and was verified only for highly refined driving situations. For real implementation of prediction based EMS, it is necessary to verify various fault conditions by external factors.

Second, it is problem of adaptability to real driving data. In this study, the prediction model was trained by using the driving cycle for authorized fuel consumption measurement. This is an example of a prediction model corresponding to the initial shipment of the vehicle. However, after the vehicle has been shipped, the prediction model must be retrained using actual driving cumulative data. There is a need to analyze the performance of the trained model with actual driving data and to identify the problems.

It is expected that the above mentioned additional studies will enhance the completeness of developed EMS.

Bibliography

[1] International Council on Clean Transportation, “Light-duty vehicle greenhouse gas and fuel economy standards, 2017 global update,” 2017.

[2] International Energy Agency, “Technology roadmap: Electric and plug-in hybrid electric vehicles, updated june 2011,” 2011.

[3] M. Ehsani, Y. Gao, S. E. Gay, and A. Emadi, Modern Electric, Hybrid Electric, and Fuel Cell Vehicles: Fundamentals, Theory, and Design. Boca Raton, FL: CRC, 2004.

[4] F. R. Salmasi, “Control Strategies for Hybrid Electric Vehicles: Evolution, Classification, Comparison, and Future Trends,” IEEE Transactions on Vehicular Technology, vol. 56, no. 5, pp. 2393–2404, 2007.

[5] S. Wirasingha and A. Emadi, “Classification and review of control strategies for plug-in hybrid electric vehicles,” 2009 IEEE Vehicle Power and Propulsion Conference, 2009.

[6] A. M. Phillips, M. Jankovic, and K. Bailey, “Vehicle system controller design for a hybrid electric vehicle,” in Proc. IEEE Int. Conf. Control Appl., Anchorage, AK, Sep. 2000, pp. 297–302.

[7] C. G. Hochgraph, M. J. Ryan, and H. L. Wiegman, “Engine control strategy for a series hybrid electric vehicle incorporating load leveling and computer controlled energy management,” SAE J. SAE/SP-96/1156, pp. 11–24, 2000.

[8] V. H. Johnson, K. B. Wipke, and D. J. Rausen, “HEV control strategy for realtime optimization off fuel economy and emissions,” in Proc. Future Car Congr., Crystal City, VA, Apr. 2000.

[9] H.-D. Lee, E.-S. Koo, S.-K. Sul, and J.-S. Kim, “Torque control strategy

for a parallel-hybrid vehicle using fuzzy logic," IEEE Ind. Appl. Mag., vol. 6, no. 6, pp. 33–38, Nov./Dec. 2000.

[10] R. Langari and J.-S. Won, "Intelligent energy management agent for a parallel hybrid vehicle—Part I: System architecture and design of the driving situation identification process," IEEE Trans. Veh. Technol., vol. 54, no. 3, pp. 925–934, May 2005.

[11] J.-S. Won and R. Langari, "Intelligent energy management agent for a parallel hybrid vehicle—Part II: Torque distribution, charge sustenance strategies, and performance results," IEEE Trans. Veh. Technol., vol. 54, no. 3, pp. 935–952, May 2005.

[12] C.-C. Lin, H. Peng, J. W. Grizzle, and J.-M. Kang, "Power management strategy for a parallel hybrid electric truck," IEEE Trans. Control Syst. Technol., vol. 11, no. 6, pp. 839–848, Nov. 2003.

[13] M. O'Keefe and T. Markel, "Dynamic programming applied to investigate energy management strategies for a plug-in HEV," Nat. Renew. Energy Lab., Golden, CO, Rep. NREL/CP-540-40376, 2006.

[14] Q. Gong and Y. Li, "Trip based power management of plug-in hybrid electric vehicle with two-scale dynamic programming," in Proc. IEEE Vehicle Power Propulsion Conf., Arlington, TX, Sep. 2007, pp. 12–19.

[15] X. Lin, A. Ivanco, and Z. Filipi, "Optimization of Rule-Based Control Strategy for a Hydraulic- Electric Hybrid Light Urban Vehicle Based on Dynamic Programming," SAE Int. J. Alt. Power., pp. 249–259, 2012.

[16] H. Lee, C. Kang, Y. Il Park, and S. W. Cha, "A study on power management strategy of HEV using dynamic programming,"World Electr. Veh. J., vol. 8, no. 1, pp. 274–280, 2016.

[17] Z. D. Asher, D. A. Baker, and T. H. Bradley, "Prediction Error Applied to Hybrid Electric Vehicle Optimal Fuel Economy," IEEE

Transactions on Control Systems Technology, vol. 26, no. 6, pp. 2121–2134, 2018.

[18] N. Kim, A. Rousseau, and D. Lee, “A jump condition of PMPbased control for PHEVs,” J. Power Sources, vol. 196, no. 23, pp. 10380–10386, 2011.

[19] N. Kim, S. Cha, and H. Peng, “Optimal control of hybrid electric vehicles based on Pontryagin’s minimum principle,” IEEE Trans. Control Syst. Technol., vol. 19, no. 5, pp. 1279–1287, 2011.

[20] N. Kim, S. W. Cha, and H. Peng, “Optimal equivalent fuel consumption for hybrid electric vehicles,” IEEE Trans. Control Syst. Technol., vol. 20, no. 3, pp. 817–825, 2012.

[21] C. Zheng, G. Xu, K. Xu, Z. Pan, and Q. Liang, “An energy management approach of hybrid vehicles using traffic preview information for energy saving,” Energy Convers. Manag., vol. 105, pp. 462–470, 2015.

[22] G. Paganelli, G. Ercole, A. Brahma, Y. Guezennec, and G. Rizzoni, “General supervisory control policy for the energy optimization of charge sustaining hybrid electric vehicles,” J. Soc. Autom. Eng. Jpn., vol. 22, no. 4, pp. 511–518, Oct. 2001.

[23] G. Paganelli, S. Delpart, T. M. Guerra, J. Rimaux, and J. J. Santin, “Equivalent consumption minimization strategy for parallel hybrid powertrains,” in Proc. IEEE/VTS Fall VTC Conf. Sponsored, Birmingham, AL, May 2002, pp. 2076–2080.

[24] S. Delpart, T. M. Guerra, and J. Rimax, “Optimal control of a parallel powertrain: From global optimization to real time control strategy,” in Proc. IEEE/VTS Spring VTC Conf., Birmingham, AL, May 2002, pp. 2082–2087.

[25] A. Sciarretta, L. Guzzella, and M. Back, “A Real-Time Optimal

Control Strategy for Parallel Hybrid Vehicles with On-Board Estimation of the Control Parameters," IFAC Proc. Vol., vol. 37, no. 22, pp. 489–494, 2004.

[26] A. Sciarretta, M. Back, and L. Guzzella, "Optimal control of parallel hybrid electric vehicles," IEEE Trans. Control Syst. Technol., vol. 12, no. 3, pp. 352–363, May 2004.

[27] L. Serrao, S. Onori, and G. Rizzoni, "ECMS as a realization of pontryagin's minimum principle for HEV control," Proc. Am. Control Conf., pp. 3964–3969, 2009.

[28] C. Musardo, G. Rizzoni, and B. Staccia, "A-ECMS: An adaptive algorithm for hybrid electric vehicle energy management," Proc. 44th IEEE Conf. Decis. Control. Eur. Control Conf. CDCECC '05, vol. 2005, no. 4–5, pp. 1816–1823, 2005.

[29] P. Pisu and G. Rizzoni, "A comparative study of supervisory control strategies for hybrid electric vehicles," IEEE Trans. Control Syst. Technol., vol. 15, no. 3, pp. 506–518, 2007.

[30] S. Onori and L. Serrao, "On Adaptive-ECMS strategies for hybrid electric vehicles," Les Rencontres Sci. d'IFP Energies Nouv. - Int. Sci. Conf. hybrid Electr. Veh. - RHEVE 2011, no. December, pp. 1–7, 2011.

[31] J. Park, Z. Chen, L. Kiliaris, M. Kuang, M. Masrur, A. Phillips, and Y. Murphey, "Intelligent Vehicle Power Control Based on Machine Learning of Optimal Control Parameters and Prediction of Road Type and Traffic Congestion," IEEE Transactions on Vehicular Technology, vol. 58, no. 9, pp. 4741–4756, 2009.

[32] W. Enang and C. Bannister, "Robust proportional ECMS control of a parallel hybrid electric vehicle," Proceedings of the Institution of Mechanical Engineers, Part D: Journal of Automobile Engineering, vol.

231, no. 1, pp. 99–119, 2016.

[33] X. Jiao, Y. Li, F. Xu, and Y. Jing, “Real-time energy management based on ECMS with stochastic optimized adaptive equivalence factor for HEVs,” Cogent Engineering, vol. 5, no. 1, 2018.

[34] B. Asadi and A. Vahidi, “Predictive Cruise Control: Utilizing Upcoming Traffic Signal Information for Improving Fuel Economy and Reducing Trip Time,” IEEE Transactions on Control Systems Technology, vol. 19, no. 3, pp. 707–714, 2011.

[35] C. Sun, X. Hu, S. J. Moura, and F. Sun, “Velocity Predictors for Predictive Energy Management in Hybrid Electric Vehicles,” IEEE Transactions on Control Systems Technology, vol. 23, no. 3, pp. 1197–1204, 2015.

[36] C. Sun, F. Sun, and H. He, “Investigating adaptive-ECMS with velocity forecast ability for hybrid electric vehicles,” Appl. Energy, vol. 185, pp. 1644–1653, 2017.

[37] J. Ziegmann, J. Shi, T. Schnorer, and C. Endisch, “Analysis of individual driver velocity prediction using data-driven driver models with environmental features,” 2017 IEEE Intelligent Vehicles Symposium (IV), 2017.

[38] J. Han, Y. Park, and D. Kum, “Optimal adaptation of equivalent factor of equivalent consumption minimization strategy for fuel cell hybrid electric vehicles under active state inequality constraints,” J. Power Sources, vol. 267, pp. 491–502, 2014.

[39] F. Tianheng, Y. Lin, G. Qing, H. Yanqing, Y. Ting, and Y. Bin, “A Supervisory Control Strategy for Plug-In Hybrid Electric Vehicles Based on Energy Demand Prediction and Route Preview,” IEEE Transactions on Vehicular Technology, vol. 64, no. 5, pp. 1691–1700, 2015.

[40] J. Han, D. Kum, and Y. Park, “Synthesis of Predictive Equivalent

Consumption Minimization Strategy for Hybrid Electric Vehicles Based on Closed-Form Solution of Optimal Equivalence Factor," IEEE Transactions on Vehicular Technology, vol. 66, no. 7, pp. 5604–5616, 2017.

국 문 초 록

하이브리드 차량의 주행 정보 기반 에너지 관리 전략에 대한 연구

서울대학교 대학원
기계항공공학부
심 재 욱

본 논문에서는 하이브리드 차량의 연비 향상을 위해 주행 정보 기반 예측 모델을 활용한 에너지 관리 전략을 제안하였다.

하이브리드 차량은 엔진과 모터를 동시에 사용하는 차량으로, 기존의 내연기관 차량에 비해 연비와 효율이 높은 대표적인 친환경 차량이다. 이러한 하이브리드 차량의 효율 향상을 위해서는 엔진과 모터를 포함한 다양한 파워트레인 구성요소를 제어하는 상위제어기의 에너지 관리 전략이 매우 중요하다. 본 연구에 사용된 등가 소모 최소화 전략은 연료의 소모량과 배터리의 전기에너지 소모량을 등가화한 등가 에너지를 고려한 실시간 최적화 기반 제어 전략이다. 등가 소모 최소화 전략은 개발이 용이하고 실시간 적용성이 좋은 편이지만, 두 에너지간의 등가화를 조정하는 등가 계수에 의해 성능이 크게 좌우된다. 특히 대부분의 최적화 기반 제어 전략과 마찬가지로, 미래의 전체 주행속도 프로파일을 알고 있을 때만이 전역 최적화된 등가계수를 알 수 있다.

본 논문에서는 특정 시간주기별로 등가계수를 변화시키는 방법을 사용하였으며, 현재시점의 주행 정보를 통해 다음 시간주기의 등가계수를 예측하는 예측 모델을 제안하였다. 예측 모델은 현재시점 주행 정보의 시계열 데이터와 이로부터 추출된 몇 개의 특성 값들을 입력받아, 다음 시간주기에 대해 최적화된 등가계수를 예측한다. 모델은 장단기 기

억 순환 신경망과 다층 신경망을 기반으로 개발되었다. 예측 모델의 학습을 위한 데이터 준비를 위해, 누적된 대량의 주행 정보를 특정 시간주기별로 나누어 각 시간주기에 대한 최적 등가계수를 시뮬레이션 기반으로 수집하였다. 수집된 데이터를 사용하여 예측모델을 학습한 후 별도의 데이터에 대하여 시험해본 결과, 예측된 계수와 최적 계수 간에 높은 상관관계가 있음을 확인하였다. 차량 시뮬레이션 검증을 위하여 학습된 예측 모델을 등가 소모 최소화 전략을 이용한 에너지 관리 전략 제어 모델과 결합하고, 차량 모델과 운전자 모델을 사용하여 전방향 시뮬레이션을 수행하였다. 연비 시험 사이클에 대한 시뮬레이션 결과 기존의 규칙기반 제어전략 대비 감소된 에너지 사용량을 보였으며, 전역 최적화된 등가계수를 사용한 경우에 보다 가까운 결과를 나타내었다.

본 논문에서 연구된 제어 전략은 주행 정보 기반의 예측모델을 활용하여 에너지 효율을 향상 시킬 수 있는 최적화 기반 제어 전략이다. 지속적인 연구를 통해 최적화 기반 제어 전략의 상용화가 가능할 것으로 기대된다.

주요어: 하이브리드 차량, 에너지 관리 전략, 등가 소모 최소화 전략, 등가 계수 예측, 주행 정보

학 번: 2017-28777